DIFFERENTIAL EQUATIONS
AND
CONTROL PROCESSES
N 1, 2023
Electronic Journal,
reg. N ΦC77-39410 at 15.04.2010
ISSN 1817-2172

http://diffjournal.spbu.ru/
e-mail: jodiff@mail.ru

Ordinary differential equations

Model map and multistability for a two predator–one prey system

G. J. Söderbacka
Åbo Akademi,
E-mail: gsoderba@abo.fi

Abstract. This work contains a review of some important results on a known two predators - one prey system. We also add essential new numerical results on multiple attractors. We consider the case when the predators coexist. We distinguish two possibilities. The first is when the dynamics is well described by the dynamics of a one dimensional map. We discuss the main behaviour of this map. For small parameter regions the map can have two attractors but no more than two. We give a numerical example, when these two attractors exist in the original three-dimensional model. The second case is when this model map is not working and something like spiral chaos often occurs. We give numerical results showing that in this case there can be at least four different attractors and discuss the behaviour of these.

Keywords: Bifurcations, chaos, multiple attractors, predator-prey.

1 Introduction

We consider a known system of n predators and one prey originally represented in [3, 4, 5] and generalized in [9]. In [11] it is shown how to rewrite it into the form

$$x_i' = \Phi_i(s)\, x_i,\;\; \Phi_i(s) = m_i \frac{s-\lambda_i}{s+a_i}, \tag{1a}$$

$$s' = \left(h(s) - \sum_{i=1}^{n} \Psi_i(s) x_i\right) s,\;\; h(s) = 1-s,\;\; \Psi_i(s) = \frac{1}{s+a_i}, \tag{1b}$$

where $i = 1, ..., n$. The system is considered only for non-negative variables and all parameters are positive.

We consider the case when $n = 2$, and we use the notations $x = x_1$ and $y = x_2$.

It is proved ([9, 2]), that in this case the set defined by $V < 1$, where $V = \frac{x}{q_1} + \frac{y}{q_2} + s$, $q_i = 1 + m_i + a_i - m_i\,\lambda_i$, is positively invariant and absorbes all solutions, where the system is defined.

Conditions for extinction of one predator and coexistence of both can be found in [9, 11]. A numerical overview of the behaviour of the system for different parameters can be found in [11].

In some case the dynamics of the system is qualitatively well modelled by a one dimensional map originally introduced in [2] and considered in [1, 10]. When this is not possible we often observe spiral-like attractors, even if up to now there is no proof how they are related to the known spiral chaos by Shilnikov.

If the one dimensional map works then there will be cyclic behaviour between the sum of predators $x + y$ and the prey s. If not the behaviour is more complicated.

We claim the one dimensional model is a good model, because all properties in the system and the dynamics of the map are observed in both and there is some correspondence in the sense that to any such system there are some maps modelling it and to any map there are some systems exposing similar behaviour. One of our aims here is to explain the main ideas of earlier works without going into technical details, in order to make it easier to understand for the reader. The other is to present new numerical results on multiple attrators.

2 The model map

Assuming λ_i, a_i small (for example λ_i, $a_i \leq 0.1$), $\frac{\lambda_2}{\lambda_1} < 1$ but not too small and m_i not too small, the dynamics can be qualitatively well described by the dynamics of iterates of a map f in the Kryzhewicz form defined as

$$f(x) = b + x - \frac{k}{1 + e^x}. \tag{2}$$

The map has been studied in [7]. Here we shortly present some results known about this map refering to the same source for details.

We consider the map in the parameter region $\{(b,k)|k < b < k/2, k < -4\}$ for other parameters either the behaviour of iterates is simple or there is an equivalent map to it in this parameter region. Here the map has two critical points and the Schwarzian is negative so there are no more than two attractors. Let $b_1 = 2\,x_c - 1 - e^{x_c}$, where x_c is the positive critical point, which is a minimum. We restrict ourselves even more to parameters in the region $P_0 = \{(b,k)|b_1 < b \leq k/2\}$, because outside this region there is a globally attracting interval, where the map behaves like a known unimodal map with only one critical point. In this region there are two attractors, but only for narrow parameter regions. But it is known that they cannot be periodic both with periods less than four. Also there cannot be more than one two periodic orbit and three periodic orbits only appear in pairs, either one stable and the other unstable or both unstable.

It is natural to define standard three intervals for symbolic dynamics, where the map is monotonic. We denote by I_m the interval $(-\infty, -x_c]$, by I_0 the interval $[-x_c,\, x_c]$ and by I_p the interval $[x_c,\, \infty)$. Further intervals $I_{j_0\, j_1\, j_2, \ldots j_p}$ consist of points such that $x \in I_{j_0}$, $f(x) \in I_{j_1}$ and $f^i(x) \in I_{j_i}$, $i = 0, 1, \ldots$.

We say that a p-periodic orbit is of type $j_1\, j_1\, j_2, \ldots\, j_p$, where each j_i is one of m, 0, or p, and $j_i = m$, if $x_i \leq -x_c$, j_i =0, if $-x_c \leq x_i < x_c$, and $j_i = p$, if $x_i \geq x_c$.

After symbol p we can get only the symbol m, and the number of consequtive m is limited by n, the smallest number such that $f^n(-x_c) > -x_c$. The fact that $0 < f' < 1$ on intervals I_m and I_p implies that there are long intervals for iterates f^n of the function, where $f' < 1$ thus making restrictions on the number of periodic orbits of a given period n.

An example, where the model map works for the original system and the original system has a three periodic and a four periodic attractor we find for

$a_1 = 0.08798$, $a2 = 0.001038$, $\lambda_1 = 0.1$, $\lambda_2 = 0.0014532$, $m_1 = m_2 = 1$.

3 Estimates used for construction of the model map

In the case the model map is working, we can prove the existence of a positively invariant set of the type $\Omega = \Omega_1 \cup \Omega_2 \cup \Omega_3 \cup \Omega_4$, where

Ω_1 is defined by the inequality $s \le \varepsilon\,\lambda_2$, $V < 1$ and $\varepsilon < 1$,

Ω_2 is defined by the inequality $x < \varepsilon_x$, $y < \varepsilon_y$, $\varepsilon\,\lambda_2 \le s \le 1 - \varepsilon_s$,

Ω_3 is defined by the inequality $s \ge 1 - \varepsilon_s$, $V < 1$, and

Ω_4 is defined by the inequality $s' < 0, x + y > d(y/x, s)$, $V < 1$.

The function d is usually complicated, chosen so that $s' < 0$, $V < 1$ at the point (x, y, s) for which $x+y = d(y/x, s)$. It is supposed that ε_x, ε_y, ε_s are small enough. Small ε_x and ε_y implies that $s' > 0$ in Ω_2. We also suppose that d is chosen so that the dynamics is described in the following way. Any trajectory starting on the surface S defined by $x+y > d(y/x, s)$, $s = \varepsilon\,\lambda_2$, $V < 1$, enters Ω_1 (where x, y decrease), from which it enters Ω_2 (where s increases), from which it enters Ω_3 (where x, y increase), from which it enters Ω_4 (where s decreases) until it again hits S. Thus there is a well defined Poincaré map on S. This map is essentially one dimensional because of strong contraction in one direction and we try here to explain (without heavy technical exact and mathematically strict estimates) why the map defined in (2) is a good approximation to the Poincaré map. We look at approximations of the trajectory in each of the sets Ω_i. We suppose the map is defined on a line $a\,x + b\,y = u_0$ in S, where a, $b \approx 1$. We know this is very realistic. We wish to explain as simple as possible the main technical details given in the original work [2] and the modification of it in [1].

We use the following notations for points on the trajectories, where it enters the next region. The initial point is given by coordinates $(x_0,\, y_0,\, \varepsilon\,\lambda_2)$. The point of leaving Ω_1 and entering Ω_2 is denoted by $(x_1,\, y_1,\, \varepsilon\,\lambda_2)$, the point of leaving Ω_2 and entering Ω_3 is denoted by $(x_2,\, y_2,\, 1 - \varepsilon_s)$, the point of leaving Ω_3 and entering Ω_4 is denoted by $(x_3,\, y_3,\, 1 - \varepsilon_s)$. The final point on S again is denoted by $(x_4,\, y_4,\, \varepsilon\,\lambda_2)$. The variable for the model map will be $v = \ln(\frac{y}{x})$ and we use the notations $v_i = \ln(\frac{y_i}{x_i})$.

Outside region Ω there is only simple dynamics or trajectories entering Ω. Similar estimates in the corresponding two dimensional predator-prey system are obtained in [6, 8]

The idea of the estimates in the four regions is simple, just calculate elementary integrals under assumption that some coordinates are zero in some terms. To get strict estimates is much more harder, even not possible in some parts and there is a need for additional assumptions or the results get only asymptotic values. Anyhow here we only discuss the main ideas. Using approximations in each of the four regions we get estimates for next v_i in terms of the previous one and the parameters. At the end we combine all these estimates in order to get the final model map in the variable v_0. Here first the main ideas shortly and after that more details.

In region Ω_1 we assume $s = 0$ in x', y' and $\frac{s'}{s}$.

In region Ω_2 we assume $x = y = 0$ in s'.

In region Ω_3 we assume $s = 1$ in x', y'.

Region 4 is more complicated. We give some details of the integrations here.

Behaviour in Ω_1. To explain the estimate in Ω_1 we use the integration techniques introduced in [2]. We use $\frac{ds}{dx} = \frac{h(s)-\Psi_1(s)x-\Psi_2(s)y}{\Phi_1(s)}\frac{s}{x}$.

Integration along the trajectory from (x_0, y_0, s_0) to (x_1, y_1, s_1), where $s_0 = s_1$ gives $0 = \int_{s_0}^{s_1} \frac{\Phi_1(s)}{s\,h(s)} ds = \int_{x_0}^{x_1} \left(\frac{1}{x} - \frac{\Psi_1(s)}{h(s)} - \frac{\Psi_2(s)}{h(s)}\frac{y}{x}\right) dx$. From $\frac{y}{x} = \frac{\Phi_1(s)}{\Phi_2(s)}\frac{dy}{dx}$ follows $\int_{x_0}^{x_1} \frac{dx}{x} = \int_{x_0}^{x_1} \frac{\Psi_1(s)}{h(s)} dx + \int_{x_0}^{x_1} \frac{\Psi_2(s)\,\Phi_1(s)}{\Phi_2(s)\,h(s)} dy$.

For $s \approx 0$ we get $\Psi_i(s) \approx \frac{1}{a_i}$, $\Phi_i(s) \approx -\frac{\lambda_i\,m_i}{a_i}$, $h(s) \approx 1$ from which follows

$$\ln\left(\frac{x_1}{x_0}\right) \approx \frac{x_1 - x_0}{a_1} + \frac{\lambda_1\,m_1}{\lambda_2\,a_1\,m_2}(y_1 - y_0)$$

Further because x_1, $y_1 \approx 0$ we obtain

$$\ln\left(\frac{x_1}{x_0}\right) \approx -\frac{x_0}{a_1} - \frac{\lambda_1\,m_1}{\lambda_2\,a_1\,m_2}\,y_0$$

Further from $\frac{x_1}{x_0} \approx e^{-\frac{\lambda_1\,m_1\,t}{a_1}}$ and $\frac{y_1}{y_0} \approx e^{-\frac{\lambda_2\,m_2\,t}{a_2}}$ follows $\frac{y_1}{y_0} \approx \left(\frac{x_1}{x_0}\right)^{\gamma}$ and $\frac{y_1}{x_1} \approx \frac{y_0}{x_0}\left(\frac{x_1}{x_0}\right)^{\gamma-1}$, where $\gamma = \frac{m_2\,\lambda_2\,a_1}{m_1\,\lambda_1\,a_2}$. With notations $v_i = \ln\left(\frac{y_i}{x_i}\right)$ we get $v_1 \approx v_0 + (\gamma - 1)(-\frac{x_0}{a_1} - \frac{\lambda_1\,m_1}{\lambda_2\,a_1\,m_2}\,y_0)$.

If we choose x_0 and y_0 from the straight line $x_0 + y_0 = u_0$ and observe $\frac{y_0}{x_0} = e^{v_0}$ we obtain $x_0 = \frac{u_0}{1+e^{v_0}}$ and $y_0 = \frac{u_0\,e^{v_0}}{1+e^{v_0}}$ and

$$v_1 \approx v_0 + \frac{(1-\gamma)\,u_0}{a_1\,(1+e^{v_0})}\left(1 + \frac{\lambda_1\,m_1}{\lambda_2\,m_2}\,e^{v_0}\right)$$

.

Behaviour in Ω_2. Next we look at estimates in Ω_2. The main idea here is to neglect the terms $\frac{x}{s+a_1}$ and $\frac{y}{s+a_2}$ in the expression for s'. We use the notations

$$\begin{array}{l} A_1 = \frac{\lambda_1+a_1}{a_1+a_1^2},\ A_2 = \frac{\lambda_1}{a_1},\ A_3 = \frac{1-\lambda_1}{1+a_1} \\ B_1 = \frac{\lambda_2+a_2}{a_2+a_2^2},\ B_2 = \frac{\lambda_2}{a_2},\ B_3 = \frac{1-\lambda_2}{1+a_2} \\ K_x(s) = m_1 + A_1 \ln(s+a_1) - A_2 \ln(s) - A_3 \ln(1-s) \\ K_y(s) = m_2 + B_1 \ln(s+a_2) - B_2 \ln(s) - B_3 \ln(1-s). \end{array}$$

In these notations we get $\ln\left(\frac{x_2}{x_1}\right) \approx K_x(s_2) - K_x(s_1)$ and $\ln\left(\frac{y_2}{y_1}\right) \approx K_y(s_2) - K_y(s_1)$ and as final estimate in v

$$v_2 \approx v_1 + K,\ K = K_y(s_2) - K_y(s_1) - K_x(s_2) + K_x(s_1)$$

.

Behaviour in Ω_3. For estimates in Ω_3 we use $s \approx 1$ we get $\Phi_i(s) \approx -\frac{(1-\lambda_i)\, m_i}{1+a_i}$ implying

$$v_3 \approx v_2 + (\alpha - 1)\ln(\frac{x_3}{x_2}),\ \alpha = \frac{m_2}{m_1}\frac{(1-\lambda_2)(1+a_1)}{(1-\lambda_1)(1+a_2)}$$

.

Behaviour in Ω_4. The estimates in Ω_4 are more difficult to explain in an easy way and we just use adding a constant K_4 so that $v_4 \approx v_3 + K_4$

Adding all estimates for v_i and supposing $\frac{x_3}{x_2} \approx \frac{x_0}{x_1}$ we get the form (2) for the estimating model map, where

$$b = K + K_4 + (\gamma - \alpha)\, u_0 \frac{\lambda_1\, m_1}{\lambda_2\, a_1\, m_2},\ k = (\gamma - \alpha)\, \frac{u_0}{a_1}\left(1 - \frac{\lambda_1\, m_1}{\lambda_2\, m_2}\right).$$

One example of graphs showing some similarity is shown in figure 1. We conjecture that for any such map there are some systems with the same behaviour, with parameters not differing much from those used to get the model.

Finally we observe that $b < k$ ($b > 0$) leads to extinction of predator y (x), thus giving better extinction conditions than in [9, 2]

4 Multistability when the model map not working

The map (2) can have no more than two attractors. But when the model map is not working there can be even more. In figure 2 we find detected periodicities of

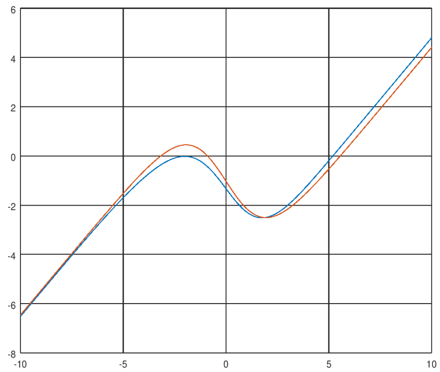

Figure 1: Graph of model map and comparison with behaviour in the original system for $\lambda_1 = 0.1$, $\lambda_2 = 0.016$, $a_1 = 0.1$, $a_2 = 0.012$, $m_1 = m_2 = 1$ and $\varepsilon = 1$, $u_0 = 1.2$. Blue for real original map and red for model map. We have chosen $K_4 \approx 1.77$.

intersections of attractors with $s = \lambda_2$, $s' < 0$. We see that regions overlap. For example when $a_1 = 1$, $a_2 = 0.0155$, four regions overlap, two different for four periodicities and one for three periodicity and the general for simple periodic attractor. In figure 4 we see parameter regions for the existence of three of the attractors and how these regions overlap. Except for these three a simple one-periodic is present in large parameter regions.

Intersections of the basins of the attractors with $s' = 0$ are shown in figures 5 and 6.

Action of Poincaré map on the points of the periodic attractors is shown in figure 7. We observe that for the Poincaré map on $s' = 0$ one four periodic attractor of $s = \lambda_2$, $s' < 0$ for the Poincaré map becomes five-periodic.

We have also found unstable periodic orbits of periods three, four and five. We give some estimates of the eigenvalues of the Jacobian matrix of the Poincaré map at the period orbits ($u = \ln(s)$):

- stable fixed point at $v = -3.302$, $u = -2.727$, eigenvalues of Jacobian matrix are about $-0.56 \pm 0.35\,i$
- stable 3-periodic point at $v = -2.523$, $u = -2.47$, eigenvalues of Jacobian matrix are about $-0.22 + 0.28\,i$
- three periodic, unstable node at $v = -3.517$, $u = -2.07916$, eigenvalues of Jacobian matrix are about 0.05 and 2.25
- stable 4 -periodic at $v = -1.9788$, $u = -2.54457$ eigenvalues of Jacobian

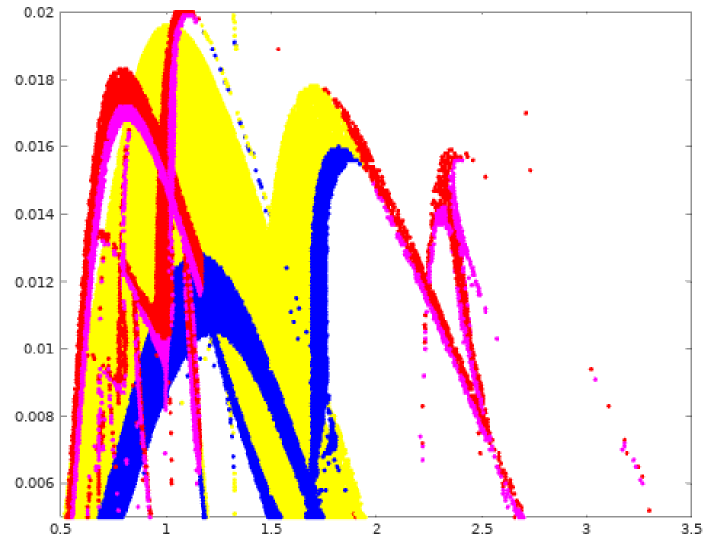

Figure 2: Detected periodicities of attractors in the case $\lambda_1 = 0.3$, $\lambda_2 = 0.2$, $m_1 = m_2 = 1$. Horiontal axis corresponds to a_1 and vertical to a_2. Yellow – 3 periodic, red - 4 periodic, blue - 6 periodic, magenta – 8 periodic. Everywhere one periodic.

matrix are about $-0.2 \pm 0.2\,i$

- unstable 4 -periodic at $v = -2.1$, $u = -2.69$ eigenvalues of Jacobian matrix are about 2.4 and 0.025
- stable 5-periodic at $v = -4.266$, $u = -1.4125$ eigenvalues of Jacobian matrix are about -0.76 and -0.08
- unstable 5-periodic at $v = -3.524$, $u = -4.138$ eigenvalues of Jacobian matrix are about -0.005 and 7.2

In figure 8 we show a bifurcation diagram of the behaviour of the ratio of the predators chosing a_1 as bifurcation parameter and keeping all other parameters constant. The four periodic jumps to the 3-periodic to the left and to the 1-periodic to the right. The five periodic jumps to the 4-periodic to the left and to the 1-periodic to the right. We observe that the five-periodic has period four when chosing the Poincaré map on $s = \lambda_2$ instead of on $s' = 0$.

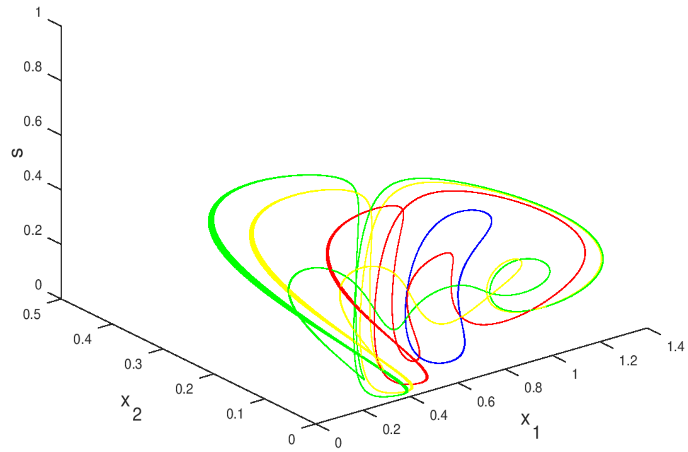

Figure 3: Four attractors in the case $\lambda_1 = 0.3$, $\lambda_2 = 0.2$, $a_1 = 1$, $a_2 = 0.0155$, $m_1 = m_2 = 1$. Green for four periodic, yellow for five periodic, red for three periodic, blue for simple one periodic. We used the following logaritmic coordinates for the initial values on the attractors:
(-0.0595, -1.91, -1.61) for simple period,
(0.0945, -3.707, -1.609), for three periodic,
(0.0886, -8.9188, -1.609) for the five periodic and
(-0.1716, -2.8988, -1.609) for the four periodic one.

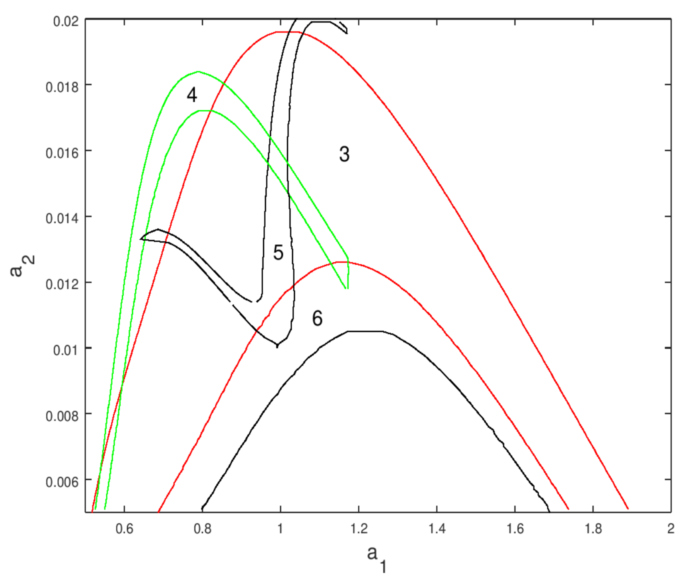

Figure 4: Some parameter regions for some periodic attractors of periods 3,4,5 and 6. Notice that there are many other such regions we do not see here.

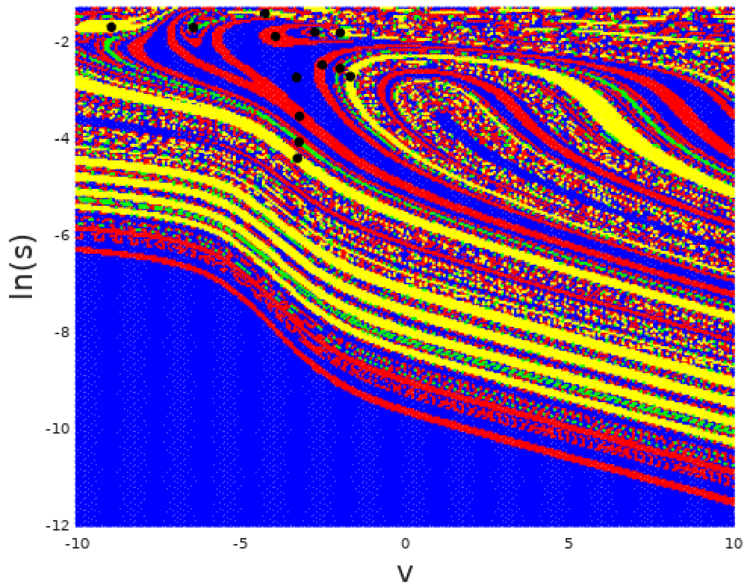

Figure 5: Basins of attractions of the four attactors in figure 3 with correponding colours. Used intersection with part of surface $s' = 0 < s"$. Black points corresponds to points on the attractors themselves.

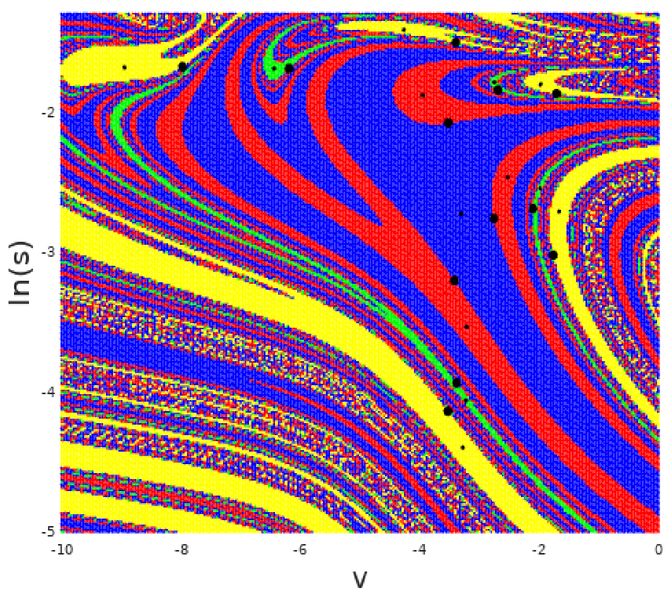

Figure 6: Magnifications of the basins of attractions of the four attactors in figure 5

References

[1] Eirola T., Osipov A. V., Söderbacka G. Chaotic regimes in a dynamical system of the type many predators one prey. Research reports A 386, Helsinki University of Technology, (1996).

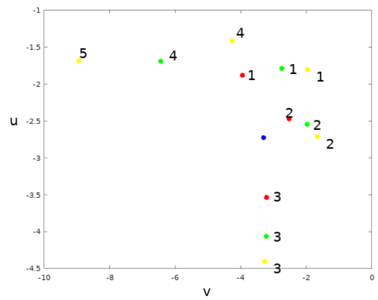

Figure 7: The order of mapping one periodic point to another for the Poincaré map, they seem to rotate around the fixed point corresponding to the simple periodic orbit.

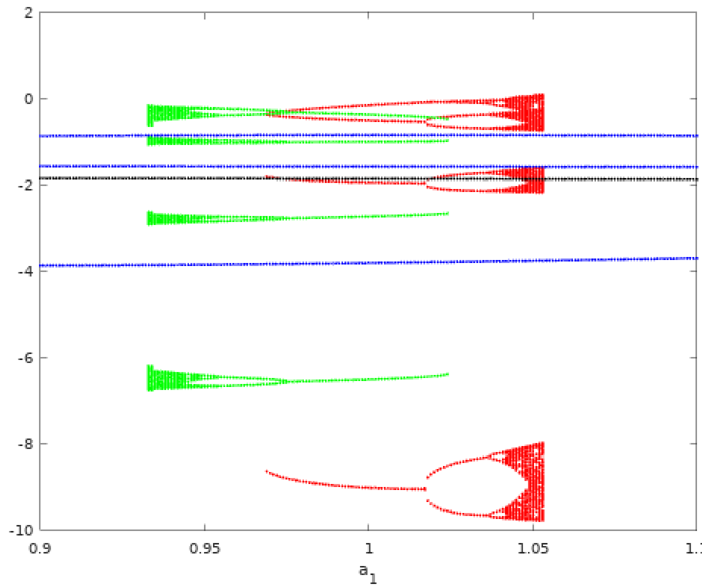

Figure 8: Bifurcation diagram, bifurcation parameter a_1, vertical axis $\ln\left(\frac{x_2}{x_1}\right)$, intersection with $s = \lambda_2$. One periodic in black, 3-periodic in blue, 4-periodic in green, 5-periodic in red (4-periodic in this place).

[2] Eirola T., Osipov A. V., Söderbacka G. On the appearance of chaotic regimes in one dynamical system of type two perdators — one prey, Actual Problems of Modern Mathematics, Boxitogorsk, 1, 39-70 (1996).

[3] Hsu B., Hubell S. P., Waltman P. Competing predators, SIAM J. Appl. Math. 35, No.4, 617-625 (1978).

[4] Hsu S. B. Limiting behaviour for competing species, SIAM J. Appl. Math. 34, No.4, 760-763 (1978).

[5] Hsu B., Hubell S. P., Waltman P. A contribution to the theory of competing predators, Ecological Monographs 48, No.3, 337-349 (1978).

[6] Hsu S.-B., Shi J. Relaxation oscillation profile of limit cycle in predator-prey system, Discrete and Continuous Dynamical Systems Series B 11, No.4, 893-911 (2009).

[7] Kryzhewich S., Avrutin V., Söderbacka G. Bistability in a one-dimensional model of a two-predators-one-prey population dynamics system, https://arxiv.org/abs/2108.06739, and Lobachevskii Journal of Mathematics, 2021, Vol. 42, No. 14, pp. 3486–3496.

[8] Lundström N. L. P., Söderbacka G. Estimates of size of cycle in a predator-prey system, Differential Equations and Dynamical Systems, DOI: 10.1007/s12591-018-0422-x (2018).

[9] A V Osipov, G Söderbacka. Extinction and coexistence of predators. Dinamicheskie sistemy, 6, 1, (2016), 55–64. http://dynsys.cfuv.ru/

[10] Osipov A V, Söderbacka G, Poincaré map construction for some classic two predators - one prey systems, *Internat. J. Bifur. Chaos Appl. Sci. Engrg*, **27**, (2017), no 8, 1750116, 9 pp.

[11] G J Söderbacka, A S Petrov. Review on the behaviour of a many predator - one prey system. *Dinamicheskie sistemy.* 2019, 9(37), No3, pp 273-288.